Articles

Protein Farnesyltransferase Inhibitors Exhibit Potent Antimalarial Activity

Laxman Nallan,[†,☆] Kevin D. Bauer,[‡,☆] Pravin Bendale,[†] Kasey Rivas,[‡] Kohei Yokoyama,[†] Carolyn P. Hornéy,[‡] Prakash Rao Pendyala,[⊥] David Floyd,[⊗] Louis J. Lombardo,[⊗] David K. Williams,[⊗] Andrew Hamilton,[#] Said Sebti,[*] William T. Windsor,[▽] Patricia C. Weber,[▽,◇] Frederick S. Buckner,[‡] Debopam Chakrabarti,[⊥] Michael H. Gelb,[†,§,*] and Wesley C. Van Voorhis[‡,||,*]

Departments of Chemistry, Medicine, Biochemistry, and Pathobiology, University of Washington, Seattle, Washington 98195, Department of Molecular Biology and Microbiology, University of Central Florida, Orlando, Florida 32826, Bristol-Myers Squibb Pharmaceutical Research Institute, Princeton, New Jersey 08543-4000, Department of Chemistry, Yale University, New Haven, Connecticut 06520, Schering-Plough Research Institute, Kenilworth, New Jersey 07033, and Departments of Oncology and Biochemisty & Molecular Biology, H. Lee Moffitt Cancer Center & Research Institute, Tampa, Florida 33612

Received November 7, 2004

New therapeutics to combat malaria are desperately needed. Here we show that the enzyme protein farnesyltransferase (PFT) from the malaria parasite *Plasmodium falciparum* (*P. falciparum*) is an ideal drug target. PFT inhibitors (PFTIs) are well tolerated in man, but are highly cytotoxic to *P. falciparum*. Because of their anticancer properties, PFTIs comprise a highly developed class of compounds. PFTIs are ideal for the rapid development of antimalarials, allowing "piggy-backing" on previously garnered information. Low nanomolar concentrations of tetrahydroquinoline (THQ)-based PFTIs inhibit *P. falciparum* PFT and are cytotoxic to cultured parasites. Biochemical studies suggest inhibition of parasite PFT as the mode of THQ cytotoxicity. Studies with malaria-infected mice show that THQ PFTIs dramatically reduce parasitemia and lead to parasite eradication in the majority of animals. These studies validate *P. falciparum* PFT as a target for the development of antimalarials and describe a potent new class of THQ PFTIs with antimalaria activity.

Introduction

Between one and two million people die annually from malaria, most from falciparum malaria, and a further 300−500 million cases occur each year.[1] Chloroquine is currently the most widespread and inexpensive drug used to treat malaria. The development of resistance to it and other agents, however, necessitates the development of new antimalarial compounds for use as monotherapy or in combination with existing methods of treatment.[1,2] An increasing number of efforts to develop antimalarial drugs have been initiated in nonprofit institutions.[1,2] Given the obvious limitations of full drug development at nonprofit institutions, we have been searching for potential opportunities to make use of chemical entities and pharmacological data from industry for rapidly developing new antimalarial drugs. This "piggy-back" drug development approach is different from the conventional one of searching for malarial drug targets that are unique to the parasite.

The enzyme protein farnesyltransferase (PFT) appears to be a promising "piggy-back" antimalarial target. PFT inhibitors have been extensively developed for anticancer therapy, and diverse compounds with drug-like properties are available.[3−5] PFT transfers the farnesyl group, a 15-carbon isoprenoid lipid unit, from farnesyl pyrophosphate (FPP) to the C-termini of a specific set of proteins, including Ras GTPase, in eukaryotic cells.[6] Farnesylation is the first in a series of posttranslational events required for the function and localization of key proteins in mammalian cells. The clinically relevant red blood cell (RBC) stages of *P. falciparum* contain PFT activity,[7,8] and searching the now complete *P. falciparum* genome sequence database[9] reveals the apparent absence of protein geranylgeranyltransferase-I (PGGT-1). The latter enzyme adds the 20-carbon geranylgeranyl group to proteins such as the γ-subunits of heterotrimeric G proteins.[6] Inhibition of both PFT and PGGT-1 is extremely toxic to mammalian cells. The apparent lack of PGGT-I in malaria suggests that inhibitors of *P. falciparum* PFT (PfPFT) might be highly toxic to parasites because vital proteins that are normally geranylgeranylated by PGGT-1 and farnesylated by PFT in mammalian cells are likely farnesylated by PfPFT in *P. falciparum*.

Chemistry. Synthesis of tetrahydroquinoline-based analogues was carried out according to Scheme 1.

The 6-cyano-1,2,3,4-tetrahydroquinolin-3-ylamine hydrochloride **1** has been prepared, as described,[10] in five steps from commercially available 3-aminoquinoline.

* Corresponding authors. W.C.V.V.: Phone 206-543-2447, fax 206-685-8681 (wesley@u.washington.edu). M.H.G.: Phone (206) 543-7142, fax 206-685-8665 (gelb@chem.washington.edu).
† Department of Chemistry, University of Washington.
‡ Department of Medicine, University of Washington.
§ Department of Biochemistry, University of Washington.
|| Department of Pathobiology, University of Washington.
⊥ University of Central Florida.
⊗ Bristol-Myers Squibb Pharmaceutical Research Institute.
Yale University.
▽ Schering-Plough Research Institute.
○ H. Lee Moffitt Cancer Center & Research Institute.
◇ Current address: Imiplex, Yardley Pennsylvania 19067.
☆ These authors contributed equally to this study.

10.1021/jm0491039 CCC: $30.25
Published on Web 05/05/2005

Scheme 1. Synthesis of Tetrahydroquinolines[a]

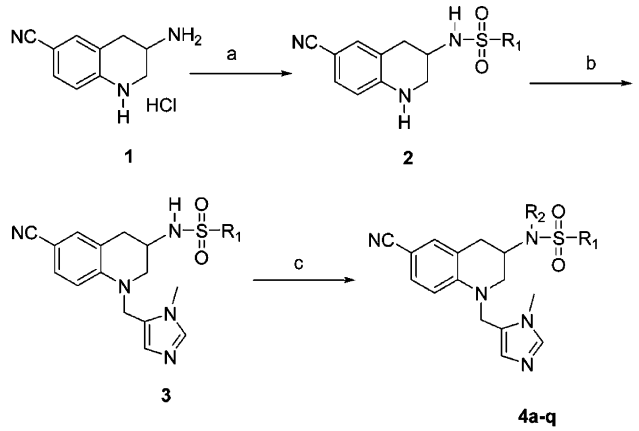

[a] Reagents and conditions: (a) R_1-SO_2Cl, DIPEA, CH_3CN; (b) 1-methyl-5-formylimidazole, dichloroethane−trifluoroacetic acid (1:1), triethylsilane; (c) R_2-Br, Cs_2CO_3, DMF.

Compound **1** was coupled with appropriate sulfonyl chloride in CH_3CN to yield the sulfonamides **2**. These sulfonamides were reacted with 1-methyl-5-formylimidazole under reductive amination conditions[11] followed by alkylation of the sulfonamide nitrogen with different alkyl halides in the presence of Cs_2CO_3 afforded target compounds (**4a**−**q**) in good yield.

Results and Discussion

We tested a variety of mammalian-cell-optimized PFTIs in clinical and pre-clinical development from Abbott (e.g. **9**−**10**),[12] Bristol-Myers Squibb (BMS) (e.g. **7**),[13] Janssen (e.g. **6**),[14] Merck (e.g. **8**),[15] Schering-Plough (e.g. **5**),[16] and Hamilton/Sebti groups (e.g. **10a**,**b**)[17] for their ability to block the in vitro growth of the intraerythrocytic forms of *P. falciparum* (Figure 1). The most potent compounds are the peptidomimetics from Hamilton/Sebti and the heterocyclics from BMS. Of the peptidomimetics, **10a** has minimal cell penetration capacity presumably because of its polar methionyl group.[18] The benzyl ester of **10a**, compound **10b**, is a prodrug that has minimal PfPFT inhibitory activity (Figure 1), presumably until it penetrates cells and is cleaved by esterases to **10a** which is a potent PfPFT inhibitor (Figure 1).[18]

We then tested a variety of PFTIs from BMS and found that the tetrahydroquinoline (THQ) series of compounds [e.g. **4a**, **4b**, and **4e**] were superior to the benzodiazepine compounds (e.g. **7**) for inhibition of PfPFT and *P. falciparum* growth in vitro (Figure 1). Indeed, the THQ **4a** displays an effective dose that inhibited 50% of *P. falciparum* 3D7 strain proliferation (ED_{50}) of 5 nM, a little less than the observed ED_{50} of chloroquine using chloroquine-sensitive strains of *P. falciparum.* Table 1 shows examples of the structure−activity of the THQs against *P. falciparum* growth and that five THQs display ED_{50}s below 8 nM using the 3D7 strain. The ED_{50} values of five of these most potent THQs against four *P. falciparum* strains (W2, K1, HB3, and Dd2) were within 4-fold of the *P. falciparum* 3D7 ED_{50} values (Table 2). These five strains represent a variety of drug resistance patterns and geographic distribution, making it likely that cross-resistance of PFTIs and antimalarials probably does not occur, and strains from all over the world are susceptible to PFTI growth inhibition.

All compounds displaying potent antimalarial activity with an ED_{50} of less than 200 nM were potent in vitro inhibitors of PfPFT, with values of IC_{50}, the concentration that blocked 50% of the enzymatic activity, in the less than 10 nM range (Figure 1 and Table 1). There was little selectivity for PfPFT vs mammalian PFT (Table 1), as expected for these mammalian-optimized PFTIs, but finding selective inhibitors was not our goal because of the relative lack of toxicity of PFTI to mammals compared with protozoa like *Plasmodium*. However, many mammalian-cell-optimized PFTIs were not effective against *P. falciparum* cell proliferation (Figure 1). There are at least two reasons for this. Some of those with ED_{50}s above 1 μM probably are unable to penetrate the multiple membranes to inhibit the malaria parasite PFT (Janssen and Abbott compounds **6**, **9**, and **10**, see evidence below supporting this for the Janssen compound **6**). Others with poor ED_{50}s have relatively poor activity against the malaria PFT enzyme (Schering-Plough and Merck compounds **5** and **8**). This explains the relatively poor correlation of IC_{50} and ED_{50} values in Figure 1. We chose to focus on the BMS THQ compounds for further studies on the correlation of PFTI and cytotoxicity because of their potency against PfPFT and *P. falciparum* cell proliferation.

Examples of the structure−activity relationships of THQ analogues are shown in Table 1 (**4m**−**o**). Varying only the sulfonamide-linked (R1) *N*-methylimidazole (**4d**) to 2-pyridyl (**4m**), 3-pyridyl (**4n**), and 4-pyridyl (**4o**) leads to a progressive loss of activity against PfPFT (IC_{50}) and a concomitant loss in the ability to block *P. falciparum* growth (ED_{50}). The R2 group, 1-bromonaphthalene (**4h** and **4k**), gave relatively poor activity against PfPFT and against *P. falciparum* parasites in vitro. These data and other examples shown in Table 1 demonstrate that minor structural variations of the THQ compounds lead to large changes in the enzyme and parasite growth arrest potency. In general we found a good correlation between THQ potency against PfPFT and ability to block malaria growth, suggesting that PfPFT is the site of action for THQ-mediated growth arrest.

We evaluated the effect of THQ PFTI **4b** on the intraerythrocytic maturation of *P. falciparum*. Synchronized cultures at the ring stage were exposed to different concentrations of the inhibitor for 72 h. The control culture matured through late trophozoite (at 24 h), schizont (segmented at 48 h) to early trophozoite (at 72 h) stages (Figure 2, panel I). Incubation of the culture with the amount of inhibitor at less than the ED_{50}, 1 nM, had no effect on the maturation of the parasite (Figure 2, panel III). In contrast, treatment with 5 and 10 nM **4b** caused severe defects in the maturation of *P. falciparum* (Figure 2, panels V and VII). Most of the parasites did not mature beyond the trophozoite stage.

We examined whether PfPFT is the antimalarial target of these THQs. Previous work showed that *P. falciparum* proteins can be radiolabeled by adding [^{3}H]-farnesol and [^{3}H]geranylgeraniol to infected red cell cultures;[7] presumably these prenols are converted within the parasite to the corresponding pyrophosphate substrates for the protein prenyltransferases. **PFTI 4a** at its ED_{50} of 5 nM led to a reduction of the labeling of the 37−75 kDa radiolabeled bands, but most of the labeling

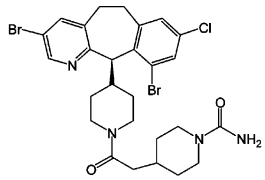

Schering-Plough
SCH 66336 **(5)**
IC_{50} > 250 nM
ED_{50} = 3,000 nM

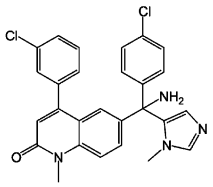

Janssen
R115777 **(6)**
IC_{50} = 17 nM
ED_{50} = 3,000 nM

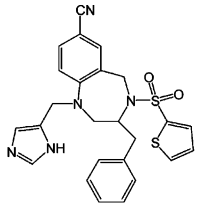

Bristol-Myers Squibb
BMS-214662 **(7)**
IC_{50} = 8 nM
ED_{50} = 180 nM

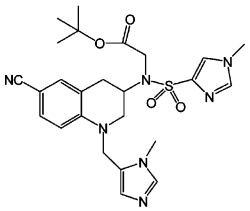

Bristol-Myers Squibb
BMS-386914 **(4a)**
IC_{50} = 0.9 nM
ED_{50} = 5 nM

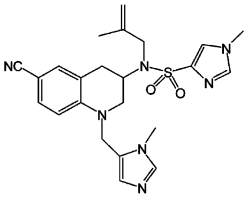

Bristol-Myers Squibb
BMS-388891 **(4b)**
IC_{50} = 0.6 nM
ED_{50} = 7nM

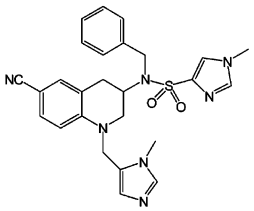

Bristol-Myers Squibb
BMS-339941 **(4e)**
IC_{50} = 0.6 nM
ED_{50} = 5 nM

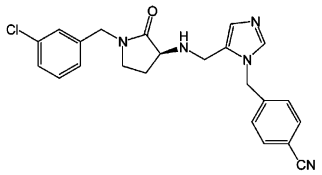

Merck
MSD-1 **(8)**
IC_{50} = 64 nM
ED_{50} >5,000 nM

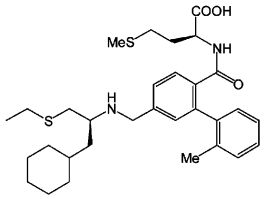

Abbott
A197574 **(9)**
IC_{50} = 5 nM
ED_{50} >5,000 nM

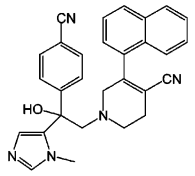

Abbott
A345677 **(10)**
IC_{50} = 9 nM
ED_{50} >5,000 nM

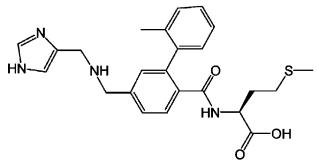

Hamilton/Sebti
FTI-2148 **(10a)**
IC50 = 15 nM
ED50 >20,000 nM

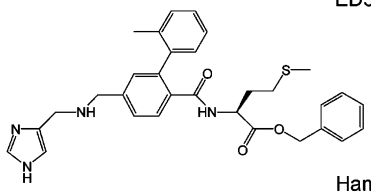

Hamilton/Sebti
Benzyl-ester-
FTI-2148 **(10b)**
IC50= 1,000 nM
ED50 = 150 nM

Figure 1. Protein farnesyltransferase inhibitors and their activity against PfPFT and *P. falciparum* growth. Shown are the structures of the PFTIs, their origin, their designator, the dose in nanomolar that inhibits 50% of the PfPFT enzyme activity (IC_{50}) or the dose in nanomolar that inhibits 50% of *P. falciparum* growth (ED_{50}).

of the 22−27 kDa bands remained (Figure 3). Increasing doses of inhibitor led to a near complete loss of radiolabeling in the 50 kDa band as well as other bands in the 37−75 kDa region. Many of the 22−27 kDa prenylated proteins are thought to be doubly geranylgeranylated rab proteins, as the *P. falciparum* genome contains a number of rab genes as well as the genes for the subunits of rab geranylgeranyltransferase-II. Note that [^{3}H]farnesol labels the 37−75 kDa proteins and the 22−27 kDa proteins, whereas [^{3}H]geranylgeraniol labels mainly the 22−27 kDa bands. This is because [^{3}H]-farnesol not only labels farnesylated *P. falciparum* proteins but also labels geranylgeranylated proteins,[7] as [^{3}H]farnesol is elongated by parasite enzymes to geranylgeranyl pyrophosphate. The faint band at 50 kDa labeled with geranylgeraniol is also reduced in the presence of the PFTI and may represent attachment of geranylgeranyl to the 50 kDa protein by PfPFT. There are at least six other visible bands that are preferentially labeled with [^{3}H]farnesol, and all are dramatically reduced by exposure to the **PFTI 4a** (Figure 3) and with **PFTI 4b** (not shown). Furthermore, we loaded the same amount of parasite protein on each gel lane and yet the reduction in radioprenylated proteins caused by addition of the THQ compound is clear. Our data show that THQ compounds kill the malaria cell at a concentration at which intracellular farnesylation is abrogated but intracellular geranylgeranylation is unabated, demonstrating that the inhibition of intracellular PFT is not simply a biochemical change in a dying parasite.

We examined the incorporation of radiolabeled farnesol into protein of parasites incubated with **6** at

Table 1. Structures and Comparative Efficacy of THQ PFTIs

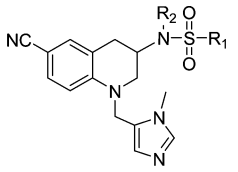

Compound	R_1	R_2	Rat-PFT IC_{50} (nM)	Pf-PFT IC_{50} (nM)	3D7 ED_{50} (nM)
4a		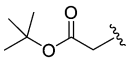	1.2	0.9	5
4b			0.7	0.6	7
4c			0.8	0.4	6
4d		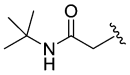	1.5	1.2	5
4e	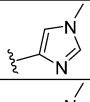	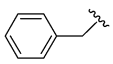	1.2	0.6	5
4f			3.4	1.5	55
4g		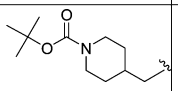	3.2	1.1	100
4h		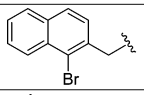	1000	28	3000
4i		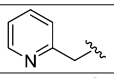	3.8	2.8	51
4j		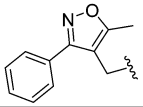	3.0	0.8	113
4k		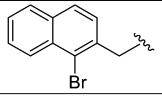	440	165	2750
4l		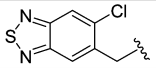	10	55	3000
4m		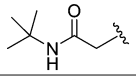	1.8	1.4	85
4n		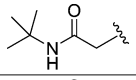	6	25	2700
4o		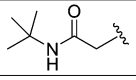	160	1000	>5000
4p	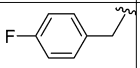	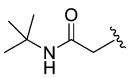	7.6	42	>5000
4q		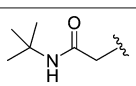	5	8	>5000

concentrations of 0.6, 1.5, and 5 times its ED_{50} (1.8 μM, 4.5 μM, and 15 μM) since this compound is a potent inhibitor of PfPFT but is poorly active at blocking malaria growth (Figure 1). These concentrations of **6** had no detectable effect on the amount of [^{3}H]-farnesol incorporated into malaria protein when examined by SDS−PAGE followed by fluorography (not shown). This shows that **6** probably does not gain entry to the cytoplasm where PfPFT resides (PfPFT IC_{50} = 7 nM), but likely inhibits growth by another mechanism. This is not surprising because the concentration of **6** needed to inhibit cell growth is nearly 1000 times higher than that of THQ compounds. The lack of change in the prenylated bands, when cell growth is inhibited by **6**,

Table 2. Sensitivity to THQ PFTIs Does Not Vary with Sensitivity or Resistance to Other Antimalarial Drugs

P. falciparum strain	origin	phenotype	ED_{50} (nM)							
			4a	**4b**	**4c**	**4d**	**4e**	ChQ[b]	Pyr[c]	Mef[d]
3D7	Africa?[a]	ChQ^S Pyr^S Mef^S	5	7	6	5	5	8	39	24
HB3	Honduras	ChQ^S Pyr^S Mef^S	7	12	10	7	10	5	2	29
W2	Indochina	ChQ^R Pyr^R Mef^S	n.d.[e]	21	14	8	14	125	n.d.	9
K1	Thailand	ChQ^R Pyr^R Mef^S	20	15	10	7	9	200	25000	10
Dd2	Indochina	ChQ^R Pyr^R Mef^R	6	10	10	4	8	78	16000	100

[a] *P. falciparum* 3D7 strain was isolated in The Netherlands near an international airport and is believed to have originated from Africa. [b] ChQ = Chloroquine (^{S} = sensitive, ^{R} = resistant). [c] Pyr = Pyrimethamine. [d] Mef = Mefloquine. [e] n.d. = not determined.

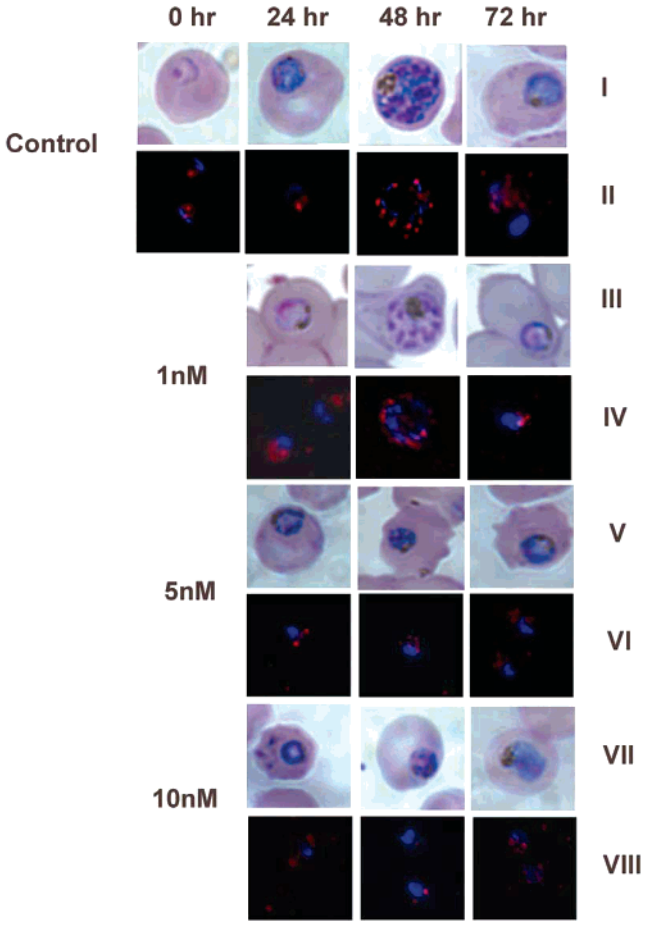

Figure 2. Effect of **PFTI 4b** on the intraerythrocytic development and localization of farnesylated proteins. The PFTI was added to synchronized *P. falciparum* 3D7 cultures at the ring stage (6 h postsynchronization). Rows I, III, V, VII: Images of thin smears of the culture at different times points. Rows II, IV, VI, VIII: At different time points, cells were fixed and probed with anti-farnesyl antibody and goat anti-rabbit IgG (red). Nuclei were stained (blue) with DAPI.

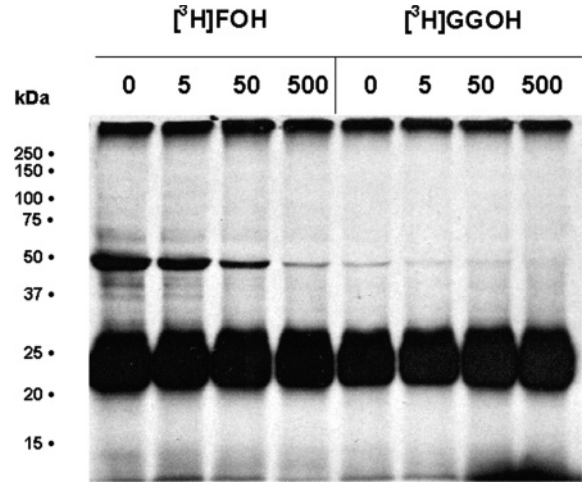

Figure 3. Inhibition of protein farnesylation by **PFTI 4a** in cultured malaria parasites. *P. falciparum* 3D7 cells in RBC were cultured in medium containing [1-^{3}H]farnesol ([^{3}H]FOH) or [1-^{3}H]geranylgeraniol ([^{3}H]GGOH) with the indicated concentration (nM) of **4a**. Parasites proteins (30 μg/lane) were resolved on a 12.5% SDS−PAGE gel and visualized by fluorography.

shows that the loss of prenylated proteins with exposure to THQ compounds is not a general biochemical effect of growth inhibition. This is further evidence that THQ compounds are targeting PFT for growth inhibition.

In a second approach to examine the mode of action of the THQs, we monitored the changes in the localization of prenylated proteins after **4b** treatment. We used an anti-farnesyl polyclonal antibody to detect farnesylated *P. falciparum* proteins by immunofluorescence microscopy. Nontreated cells show distinct foci of localization of farnesylated proteins, particularly in the schizont stage (Figure 2, panel II 48 h). The schizont stage is characterized by merozoites budding from a residual cytoplasmic mass. Each focus of farnesylated protein is within an individual merozoite. Treatment with a sub-ED_{50} concentration of **4b** (1 nM) was without effect (Figure 2, panel IV). In contrast, 5 and 10 nM of the PFTI led to a noticeable inhibition of protein farnesylation as is evident from a reduction of fluorescent spots (Figure 2, panels VI and VIII). Thus, by two independent methods, we show that treatment of *P. falciparum* with THQ-based PFTIs leads to inhibition of protein farnesylation in vivo at doses that correlate with growth inhibition. In other work, exposure of 10^8 *P. falciparum* Dd2 strain to PFTI **4b** led to selection of *P. falciparum* clones that have an increase of 12-fold in their ED_{50} to **4b**.[19] This was accompanied by a single mutation corresponding to the active site of PfPFT that led to an increase in the Ki for PFTI **4b**.[19] All together, these results strongly support PfPFT as the antimalarial target of the THQs.

We investigated whether the PFTIs are cidal versus static to *P. falciparum*. Growing parasites were exposed to 3 × ED_{50} (22.5 nM) and 30 × ED_{50} (225 nM) concentrations of **4b** followed by washing the parasites every 24 h to remove the PFTI. Asynchronous parasites were used to simulate the infection in nonimmune individuals. Parasites that were exposed to 30 × ED_{50} of **4b** failed to grow after 96 h (Figure 4). *P. falciparum* was clearly inhibited by 30 × ED_{50} of **4b** after 48 and 72 h of exposure, though some viable parasites grew after a delay. Exposure of parasites to 3 × ED_{50} of **4b** caused a delay of growth of *P. falciparum,* but viable parasites eventually grew after 96 h of exposure (Figure 4). These data show that the PFTI acts as a cidal agent with sufficient exposure, and parasite killing requires

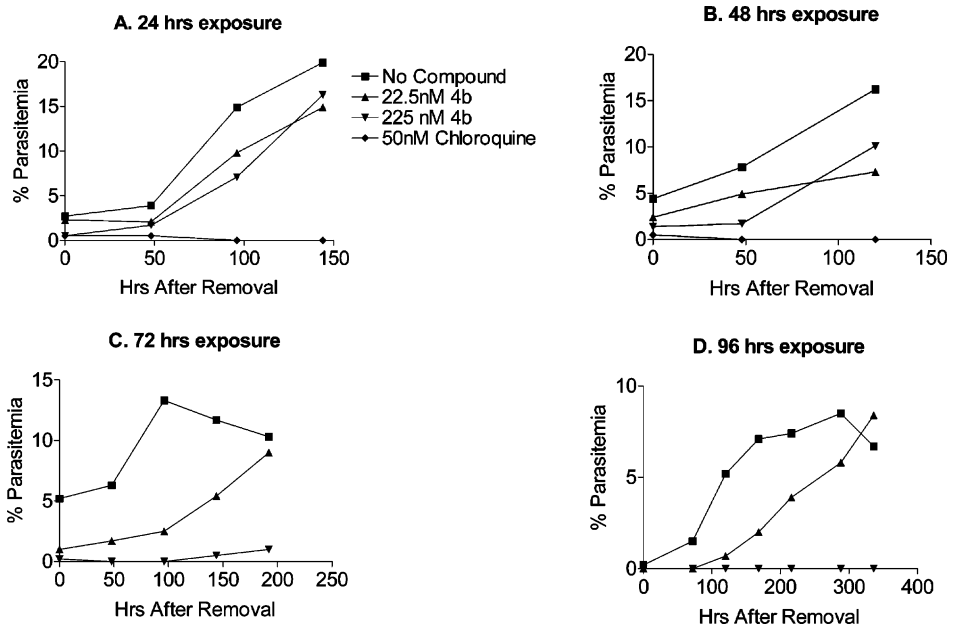

Figure 4. Varying the length of exposure of PFTI demonstrates that 96 h exposure kills *P. falciparum*. *P. falciparum* 3D7 in RBC cultures were exposed to 22.5 or 225 nM of **PFTI 4b** for varying lengths of time before washing the parasites free of drug and reculturing to test if the parasites are viable. A no drug treated control was included.

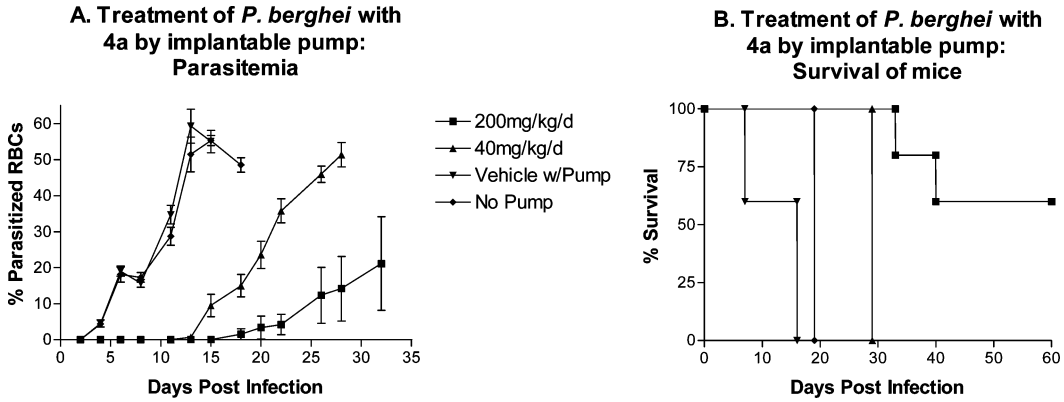

Figure 5. Treatment of *P. berghei*-infected mice with PFTI 4a leads to attenuation of infection. Osmotic pumps to deliver 200 mg/kg/day or 40 mg/kg/day of the THQ **PFTI 4a** were implanted into mice. Four hours later, mice were infected with *P. berghei*-infected RBC by IP injection. Mice with no pumps implanted or with pumps that delivered only vehicle served as controls. Mice were monitored for parasitemia (A) and mortality (B).

exposure to the inhibitor between 72 and 96 h with doses between 3 × ED_{50} and 30 × ED_{50}.

The emergence of parasites from cultures after 72 h exposure to 30 × ED_{50} suggests that THQ PFTIs are killing via a slow mechanism, compared with quinoline drugs such as chloroquine and quinine or artemesinin drugs which kill rapidly. The apparent slow action of PFTIs may be due to the relatively slow turnover of preexisting prenylated proteins. It may take some time for the pool of nonprenylated protein to fall below a critical concentration. Some malaria drugs in use also kill slowly, notably tetracyclines and clindamycin. However, these drugs are useful when combined with rapidly killing agents to achieve complete eradication, ensure cure, and prevent or delay the emergence of drug resistance.

To further explore whether the THQ PFTIs could be further developed as antimalarial drugs, we employed the *P. berghei* mouse model of malaria. As a first step, we extracted PFT from *P. berghei* and showed that it was highly susceptible to inhibition by **PFTI 4a** (IC_{50} = 0.4 nM). Mice were exposed to THQ PFTIs via implantable osmotic pumps to deliver a controlled and constant amount of drug. This approach has the advantage that one can explore the in vivo efficacy of the THQ compounds prior to optimization of compounds for desirable pharmacokinetic properties. Mice were then infected with *P. berghei*, with parasitemia and serum THQ levels periodically quantified. Dosing with pumps calculated to deliver 40 mg/kg/day and 200 mg/kg/day of **4a** led to delayed onset of parasitemia, and in the case of the higher dose, eradication of parasitemia from 60% of mice (Figure 5). Blood levels of **4a** were constant on days 2, 4, and 6 after pump implantation and were 2.24 μM ± 0.62 μM for the mice with 200 mg/kg/day pumps and 0.75 μM ± 0.22 μM for mice with the 40 mg/kg/day pumps. No toxicity was observed in any of the THQ-treated animals. Thus, exposure to the THQ PFTI led to attenuation or eradication of *P. berghei* infection. The *P. berghei* model is very demanding, in that seemingly every parasite must be eliminated or fatal parasitemia is recrudescent. In fact, comparator drugs

artesunate, artemether, and chloroquine that are effective in humans yield late onset parasitemia and death in the *P. berghei* model.[20] In our hands, even with the high dose of 10 mg/kg of chloroquine delivered orally twice daily for 3 days, only 40% of mice had their parasites apparently eradicated (data not shown). The other 60% of mice had *P. berghei* parasitemia recur a week after treatment. Thus, the finding that 60% of mice survive and have no infection at 60 days is strong evidence that the THQ PFTI is able to eradicate all of the parasites in the majority of mice.

In summary, we have validated PfPFT as a target for the development of antimalarials. PFTIs represent an extensively developed set of anticancer compounds, and extending their use for the treatment of malaria has obvious advantages when compared to studying malarial drug targets whose inhibitors must be developed by lengthy medicinal chemistry trials. We are not seeking PfPFT-specific inhibitors since clinical trials have shown that patients tolerate several different classes of mammalian PFT inhibitors well over several weeks of treatment.[5] This plus the fact that malaria patients are treated with antimalarials for <1 week argues that PFT inhibitors that are specific for the malaria enzyme are not required. The THQ compounds are a reasonable starting point for a malaria drug because they are highly potent against *P. falciparum*. We observed no toxicity in animals treated with THQs at levels that led to the eradication of *P. berghei*. Furthermore, they can be prepared by a relatively short synthetic route and are thus expected to have cost of goods desired for a drug to be used in developing countries. Efforts are now underway to explore and optimize the oral bioavailability and pharmacokinetic properties of the THQ-based PFTIs in an effort to discover a drug candidate that can be taken into human trials.

Since we have completed these studies, Wiesner et al. have reported a series of piperazinyl PFTIs are effective in inhibiting *P. falciparum* in vitro and that this growth inhibition correlated with reduction of a 50 kDa band labeling with radiolabeled farnesol.[21] In addition, these authors were also able to show efficacy in the mouse *P. berghei* model when their compounds were injected intraperitoneally.[21] These studies support our results that suggest PFTI cause growth inhibition by acting on *Pf*PFT.

Experimental Section

Chemistry. Methods and Reagents. Unless otherwise indicated, all anhydrous solvents were commercially obtained and stored in sure-seal bottles under nitrogen. Anhydrous reactions were performed under an atmosphere of dry nitrogen or argon in oven-dried glassware and were monitored for completeness by thin-layer chromatography (TLC) using silica gel 60 F-254 (0.25 mm) plates (visualized with UV light). Proton NMR spectra were recorded in $CDCl_3$, CD_3OD, or DMSO-d_6 at 300 or 500 MHz. Chemical shifts are reported in parts per million (δ) downfield from tetramethylsilane (TMS). Coupling constants (J) are reported in Hz throughout. Mass spectral data were acquired on a Bruker Esquire LC00066. The purity of selected key compounds (**4a**, **4b**, **4d**, **4e**, **4m**, **4n**, and **4o**) was assessed by high-resolution mass spectroscopy and for all compounds (**4a**−**q**) was confirmed twice by HPLC with different solvent systems. Method 1: 30 min run using a gradient of 20% to 100% methanol/water containing 0.05% trifluoroacetic acid, flow rate 12 mL/min, at room temperature on a YMC S5 ODS column (20 × 100 mm, Waters Inc.). Method 2: 30 min run on Varian Prep Star using a gradient of (20% to 100% acetonitrile/water containing 0.05% trifluoroacetic acid, flow rate 12 mL/min) at room temperature. The UV absorbance was measured at 254 nm.

Four compounds, cited in Figure 1, were obtained as a generous gift from Schering-Plough (**5**), Merck (**8**), and Abbott Laboratories (**9** and **10**). Compound **7** was prepared from commercially available D-phenylalanine methyl ester HCl and bromoisatoic anhydride according to the literature procedure.[13] Compound **6** was obtained from 4-nitrobenzoyl chloride and chlorobenzene using the known protocols.[22] Compounds **10a** and **10b** were synthesized as previously described.[23]

Synthesis of Tetrahydroquinoline-Based Inhibitors. General Procedure for Sulfonation. A solution of, for example, 6-cyano-1,2,3,4-tetrahydroquinolin-3-ylamine hydrochloride[10] (5 mmol), sulfonyl chloride[24] (10 mmol), and *N*,*N*-diisopropylethylamine (15 mmol) and 25 mL of anhydrous CH_3CN was stirred at room temperature. After stirring overnight, a light colored precipitate was isolated by vacuum filtration or on a silica gel column eluting with 50% EtOAc/hexane, affording the corresponding product as a white foam (85−95%).

1-Methyl-1*H*-imidazole-4-sulfonic Acid (6-Cyano-1,2,3,4-tetrahydroquinolin-3-yl)amide. ^{1}H NMR (500 MHz, DMSO-d_6) δ 7.80 (s, 1H), 7.78 (s,1H), 7.70 (br s, 1H), 7.25 (d, J = 8.7 Hz, 1H), 7.20 (s, 1H), 6.81 (s, 1H), 6.51 (d, J = 8.6 Hz, 1H), 3.92−4.0 (m, 1H), 3.78 (s, 3H) 3.34 (dd, J = 2.7, 11.8 Hz, 1H), 3.21 (ddd, J = 2.1, 4.4, 12.3 Hz, 1H), 2.89 (dd, J = 4.1, 16.5 Hz, 1H), 2.73 (ddd, J = 2.1, 4.8, 16.2 Hz, 1H), MS (EI) *m/z* 318.5 (M^+)

Pyridine-2-sulfonic Acid (6-Cyano-1,2,3,4-tetrahydroquinolin-3-yl)amide. ^{1}H NMR (300 MHz, CD_3OD) δ 8.51 (d, J = 7.2 Hz, 1H), 8.02 (td, J = 2.1, 7.8 Hz, 1H), 7.92 (dt, J = 1.8, 7.5 Hz, 1H), 7.47 (ddd, J = 1.2, 4.8, 7.5 Hz, 1H), 7.12 (dd, J = 2.1, 8.4 Hz, 1H), 7.0 (d, J = 1.8 Hz, 1H), 6.30 (d, J = 8.4 Hz, 1H), 5.87 (d, J = 7.8 Hz, 1 H), 3.94−4.01 (m, 1H), 3.36 (dd, J = 2.7, 12 Hz, 1H), 3.25 (ddd, J = 2.1, 4.5, 12.3 Hz, 1H), 2.87 (dd J = 4.2, 16.5 Hz, 1H), 2.71 (ddd, J = 2.1, 4.8, 16.5 Hz, 1H). MS (EI) *m/z* 315 (M^+)

General Procedure for Reductive Amination. A mixture of the sulfonamide (5 mmol), 1-methyl-1*H*-imidazole-5-carbaxaldehyde (10 mmol), and 20 mL of 50% trifluoroacetic acid in dichloroethane was warmed at 50 °C under argon. After 2 h triethylsilane (20 mmol) was added. After 48 h, the solvents were removed under reduced pressure, and the crude product was partition between methylene chloride and 1 N NaOH (45 mL). The organic layer was separated, and the aqueous layer was extracted with CH_2Cl_2 (3 × 25 mL). The combined organic layers were dried over $MgSO_4$, filtered, and concentrated. The crude residue was either recrystallized with dichloromethane or purified on a flash silica gel column.

Pyridine-2-sulfonic Acid [6-Cyano-1-(3-methyl-3*H*-imidazol-4-ylmethyl)-1,2,3,4-tetrahydroquinolin-3-yl]-amide. Flash column chromatography eluting with 1:4 v/v methanol−ethyl acetate afforded the product (68%). ^{1}H NMR (300 MHz, DMSO-d_6) δ 8.70 (d, J = 4.8 Hz, 1H), 8.14 (d, J = 6.6 Hz, 1H), 8.06 (dt, J = 1.8, 7.5 Hz, 1H), 7.99 (s, 1H), 7.67 (ddd, J = 1.2, 4.8, 7.8 Hz, 1H), 7.37 (dd, J = 2.1, 8.7 Hz, 1H), 7.27 (d, J = 1.8 Hz, 1H), 6.88 (s, 1H), 6.8 (d, J = 8.7 Hz, 1H), 4.62 (d, J = 16.5 Hz, 1H), 4.59 (d, J = 16.5 Hz, 1H), 3.85−3.73 (m, 1H), 3.60 (s, 3H), 3.38 (dd, J = 2.4, 11.7 Hz, 1H), 3.17 (dd, J = 8.7, 12.9 Hz, 1H), 2.88 (dd, J = 4.2, 15.9 Hz, 1H), 2.70 (dd, J = 8.7, 15.9 Hz, 1H). MS (EI) *m/z* 409.3 (M^+).

1-Methyl-1*H*-imidazole-4-sulfonic Acid [6-Cyano-1-(3-methyl-3*H*-imidazol-4-ylmethyl)-1,2,3,4-tetrahydroquinolin-3-yl]amide Trifluoroacetate Salt. Recrystallized by CH_2Cl_2, afforded the product as a white solid (70%) ^{1}H NMR (300 MHz, CD_3OD) δ 8.89 (s,1H), 7.82 (s, 1H), 7.72 (s, 1H), 7.41 (s, 1H), 7.36 (d, J = 8.2 Hz, 1H,), 7.22 (s, 1H), 6.80 (d, J = 8.6 Hz, 1H), 4.72 (d, J = 16.5 Hz, 1H), 4.61 (d, J = 16.5 Hz, 1H), 3.89 (s, 3H), 3.85−3.73 (m, 1H), 3.70 (s, 3H), 3.41 (dd, J = 2.2, 11.4 Hz, 1H), 3.19 (dd, J = 8.6, 12.8 Hz, 1H), 2.85 (dd, J = 4.1, 16.0 Hz, 1H), 2.74 (dd, J = 8.4, 15.7 Hz, 1H), MS (EI) *m/z* 412.5 (M^+).

***N*-[6-Cyano-1-(3-methyl-3*H*-imidazol-4-ylmethyl)-1,2,3,4-tetrahydroquinolin-3-yl]-4-fluoro-benzenesulfonamide** ^{1}H NMR (500 MHz, CD_3OD) δ 8.35 (s, 1H), 7.95−7.93 (m, 2H), 7.46 (s, 1H), 7.39 (d, J = 8.5 Hz, 1H), 7.35 (t, J = 8.0 Hz, 2H), 7.24 (s, 1H), 6.82 (d, J = 8.5 Hz, 1H), 4.82 (d, J = 17.0 Hz, 1H), 4.65 (d, J = 17.0 Hz, 1H), 3.95−3.85 (m, 4H), 3.69−3.65 (m, 1H), 3.55−3.45 (m, 1H), 2.97−2.96 (m, 1H), 2.71−2.61 (m, 1H), MS (EI) *m/z* 426.12 (M^+).

General Procedure for N-Alkylation. To a suspension of the reductive amination product (5 mmol) and Cs_2CO_3 (9.8 mmol) in dry DMF (5 mL) was added the appropriate alkyl halide (5.4 mmol), and the mixture was stirred at room-temperature overnight under argon. After addition of water (20 mL), the solution was extracted with ethyl acetate (3 × 20 mL). The organic layer was extracted with brine (3 × 10 mL). The combine organic layers were dried over $MgSO_4$ and evaporated under reduce pressure. The residue was purified by RP HPLC. Appropriate fractions were collected, and the pure product was obtained as the trifluoroacetate salt.

[[6-Cyano-1-(3-methyl-3*H*-imidazol-4-ylmethyl)-1,2,3,4-tetrahydroquinolin-3-yl]-(1-methyl-1*H*-imidazole-4-sulfonyl)-amino]-acetic Acid *tert*-Butyl Ester (4a). ^{1}H NMR (300 MHz, $CDCl_3$) δ 8.66 (s, 1H), 7.60 (s, 1H), 7.45 (s, 1H), 7.38 (d, J = 8.5 Hz, 1H), 7.16 (s, 1H), 7.12 (s, 1H), 6.65 (d, J = 8.6 Hz, 1H), 4.71 (d, J = 16.8 Hz, 1H), 4.68 (d, J = 16.8 Hz, 1H), 4.50−4.34 (m, 2H), 3.96 (d, J = 17.3 Hz, 1H), 3.90 (s, 3H), 3.81 (s, 3H), 3.44−3.55 (m, 2H), 3.12 (dd, J = 11.5, 15.2 Hz, 1H) 2.81 (dd, J = 3.2, 15.1 Hz, 1H), 1.35 (s, 9H); high-resolution mass spectroscopy (FAB+) *m/z* calcd for $C_{25}H_{32}O_4N_7S$ (MH^+) 526.2237 obsd 526.2241.

1-Methyl-1*H*-imidazole-4-sulfonic Acid [6-Cyano-1-(3-methyl-3*H*-imidazol-4-ylmethyl)-1,2,3,4-tetrahydroquinolin-3-yl]-(2-methylallyl)amide (4b). ^{1}H NMR (300 MHz, $CDCl_3$) δ 8.63 (s, 1H), 7.62 (s, 1H), 7.45 (s, 1H), 7.40−7.35 (m, 2H), 7.14 (s, 1H), 6.68 (d, J = 8.6 Hz, 1H), 5.05−4.95 (m, 1H), 4.92−4.85 (m, 1H), 4.74 (d, J = 16.7 Hz, 1H), 4.67 (d, J = 16.5 Hz, 1H), 4.48−4.21 (m, 2H), 3.99 (d, J = 17.3 Hz, 1H), 3.92 (s, 3H), 3.85 (s, 3H), 3.53−3.41 (m, 2H), 3.09 (dd, J = 11.4, 15.1 Hz, 1H) 2.9 (dd, J = 3.1, 15.0 Hz, 1H), 1.81 (s, 3H); high-resolution mass spectroscopy (FAB+) *m/z* calcd for $C_{23}H_{28}O_2N_7S$ (MH^+) 466.2025 obsd 466.2029.

1-Methyl-1*H*-imidazole-4-sulfonic Acid (2-Bromoallyl)-[6-cyano-1-(3-methyl-3*H*-imidazol-4-ylmethyl)-1,2,3,4-tetrahydroquinolin-3-yl]amide (4c). ^{1}H NMR (300 MHz, $CDCl_3$) δ 8.64 (s, 1H), 7.63 (s, 1H), 7.46 (s, 1H), 7.41−7.36 (m, 2H), 7.15 (s, 1H), 6.70 (d, J = 8.6 Hz, 1H), 6.08−6.02 (m, 1H), 5.70−5.60 (m, 1H), 4.67 (d, J = 16.5 Hz, 1H), 4.58−4.2 (m, 2H), 3.92 (s, 3H), 3.89 (m, 1H), 3.85 (s, 3H), 3.53−3.41 (m, 2H), 3.09 (dd, J = 11.4, 15.1 Hz, 1H) 2.9 (dd, J = 3.1, 15.0 Hz, 1H) MS (EI) *m/z* 531.41 (M^+).

***N-tert*-Butyl-2-[[6-cyano-1-(3-methyl-3*H*-imidazol-4-ylmethyl)-1,2,3,4-tetrahydroquinolin-3-yl]-(1-methyl-1*H*-imidazole-4-sulfonyl)amino]acetamide (4d).** ^{1}H NMR (500 MHz, CD_3OD) δ 8.94 (s, 1H), 7.83 (s, 1H), 7.79 (s, 1H), 7.43 (s, 1H), 7.39 (d, J = 8.7 Hz, 1H), 7.29 (s, 1H), 6.83 (d, J = 8.5 Hz, 1H), 4.80 (d, J = 16.7 Hz, 1H), 4.68 (d, J = 16.7 Hz, 1H), 4.32−4.41 (m, 1H), 4.01 (d, J = 17.3 Hz, 1H), 3.96 (d, J = 17.4 Hz, 1H), 3.85 (s, 3H), 3.65 (s, 3H), 3.57−3.51 (m, 2H), 3.13 (dd, J = 12, 15.1 Hz, 1H) 2.85 (dd, J = 3.3, 15.3 Hz, 1H), 1.37 (s, 9H); high-resolution mass spectroscopy (FAB+) *m/z* calcd for $C_{25}H_{33}O_4N_8S$ (MH^+) 525.2396 obsd 525.2397.

1-Methyl-1*H*-imidazole-4-sulfonic Acid Benzyl-[6-cyano-1-(3-methyl-3*H*-imidazol-4-ylmethyl)-1,2,3,4-tetrahydroquinolin-3-yl]amide (4e). ^{1}H NMR (300 MHz, CD_3OD) δ 8.85 (s, 1H), 7.94 (s, 1H), 7.75 (s, 1H), 7.45−7.21 (m, 6H), 7.14 (s, 1H), 6.72 (d, J = 8.6 Hz, 1H), 4.70−4.25 (m, 5H), 4.00 (d, J = 17.3 Hz, 1H), 3.72 (s, 3H), 3.65 (s, 3H), 3.53−3.41 (m, 1H), 3.08 (dd, J = 11.5, 15.2 Hz, 1H) 2.85 (dd, J = 3.0, 15.1 Hz, 1H); high-resolution mass spectroscopy (FAB+) *m/z* calcd for $C_{26}H_{28}O_2N_7S$ (MH^+) 502.2055 obsd 502.2022.

1-Methyl-1*H*-imidazole-4-sulfonic Acid [6-Cyano-1-(3-methyl-3*H*-imidazol-4-ylmethyl)-1,2,3,4-tetrahydroquinolin-3-yl]-(2-methylbenzyl)amide (4f). ^{1}H NMR (500 MHz, CD_3OD) δ 8.89 (s, 1H), 7.84 (s, 1H), 7.73 (s, 1H), 7.46 (s, 1H), 7.33 (d, J = 8.5 Hz, 1H), 7.28−7.18 (m, 4H), 7.12 (s, 1H), 6.70 (d, J = 8.5 Hz, 1H), 4.57−4.38 (m, 5H), 3.81 (s, 3H), 3.78 (s, 3H), 3.45 (d, J = 10 Hz, 1H), 3.25−3.20 (m, 1H), 3.02−2.97 (m, 1H), 2.89 (d, J = 13.5, 1H), 2.22 (s, 3H), MS (EI) *m/z* 516.61 (M^+).

4-{[[6-Cyano-1-(3-methyl-3*H*-imidazol-4-ylmethyl)-1,2,3,4-tetrahydroquinolin-3-yl]-(1-methyl-1*H*-imidazole-4-sulfonyl)amino]methyl}-piperidine-1-carboxylic Acid *tert*-Butyl Ester (4g). ^{1}H NMR (500 MHz, CD_3OD) δ 8.94 (s, 1H), 7.82 (s, 1H), 7.80 (s, 1H), 7.45 (s, 1H), 7.36 (d, J = 8.7 Hz, 1H), 7.29 (s, 1H), 6.75 (d, J = 8.5 Hz, 1H), 4.77 (d, J = 16.7 Hz, 1H), 4.65 (d, J = 16.7 Hz, 1H), 4.42−4.31 (m, 1H), 4.17−4.01 (m, 2H), 3.95 (s, 3H), 3.85 (s, 3H), 3.65−3.45 (m, 3H), 3.25−2.95 (m, 3H) 2.85−2.68 (m, 1H), 1.95−1.68 (m, 3H), 1.47 (s, 9H), 1.20−0.98 (m, 2H), MS (EI) *m/z* 609.5 (M^+).

1-Methyl-1*H*-imidazole-4-sulfonic Acid (1-Bromonaphthalen-2-ylmethyl)-[6-cyano-1-(3-methyl-3*H*-imidazol-4-ylmethyl)-1,2,3,4-tetrahydroquinolin-3-yl]amide (4h). ^{1}H NMR (500 MHz, CD_3OD) δ 8.85 (s, 1H), 8.30−8.20 (m, 1H), 7.98−7.74 (m, 3H), 7.71−7.48 (m, 6H), 7.25−7.18 (m, 2H), 6.62 (d, J = 8.5 Hz, 1H), 4.80−4.38 (m, 5H), 4.12 (m, 1H), 3.81 (s, 3H), 3.78 (s, 3H), 3.45 (m, 1H), 3.25−3.20 (m, 1H), 3.02−2.97 (m, 2H), MS (EI) *m/z* 632.21 (M^+).

Pyridine-2-sulfonic Acid [6-Cyano-1-(3-methyl-3*H*-imidazol-4-ylmethyl)-1,2,3,4-tetrahydroquinolin-3-yl]-pyridin-2-ylmethylamide (4i). ^{1}H NMR (300 MHz, CD_3OD) δ 8.91 (s, 1H), 8.76 (d, J = 4.8 Hz, 1H), 8.54 (d, J = 5.1 Hz, 1H), 7.98−8.15 (m, 3H), 7.83 (d, J = 7.8 Hz, 1H), 7.71 (ddd, J = 1.2, 4.5, 7.2 Hz, 1H), 7.55−7.59 (m, 1H), 7.31−7.33 (m, 2H), 7.22 (s, 1H), 6.72 (d, J = 8.7 Hz, 1H), 4.82 (d, J = 17.7 Hz, 1H), 4.76 (d, J = 17.7 Hz, 1H), 4.54−4.65 (m, 3H), 3.86 (s, 3H), 3.45−3.56 (m, 2H), 3.13 (dd, J = 10.2, 15.6 Hz, 1H), 2.93 (dd, J = 4.2, 16.2 Hz, 1H); MS (EI) *m/z* 500.3 (M^+)

Pyridine-2-sulfonic Acid [6-Cyano-1-(3-methyl-3*H*-imidazol-4-ylmethyl)-1,2,3,4-tetrahydroquinolin-3-yl]-(5-methyl-3-phenylisoxazol-4-ylmethyl)amide (4j). ^{1}H NMR (300 MHz, CD_3OD) δ 8.93 (s, 1H), 8.71 (d, J = 7.2 Hz, 1H), 8.05 (td, J = 1.8, 7.5 Hz, 1H), 7.93−8.00 (m, 1H), 7.66 (ddd, J = 1.2, 4.8, 7.5 Hz, 1H), 7.40−7.51 (m, 5 H), 7.39 (dd, J = 1.5, 8.4 Hz, 1H), 7.33 (s, 1H), 7.02 (s, 1H), 6.80 (d, J = 9.7 Hz, 1H), 4.49−4.73 (m, 4H), 4.03−4.21 (m, 1H), 3.85 (s, 3H), 3.28−3.47 (m, 2H), 2.85−2.91 (m, 1H), 2.64 (s, 3H), 2.46−2.53 (m, 1H); MS (EI) *m/z* 580.4 (M^+).

Pyridine-2-sulfonic Acid (1-Bromonaphthalen-2-ylmethyl)-[6-cyano-1-(3-methyl-3*H*-imidazol-4-ylmethyl)-1,2,3,4-tetrahydroquinolin-3-yl]amide (4k). ^{1}H NMR (300 MHz, $CDCl_3$) δ 8.79 (d, J = 7.2 Hz, 1H), 8.27−8.28 (m, 2H), 8.00−8.06 (m, 2 H), 7.85−7.93 (m, 3H), 7.62−7.68 (m, 3 H), 7.30−7.33 (m, 1H), 7.19 (s, 1H), 7.13 (s, 1H), 6.51 (d, J = 8.7 Hz, 1H), 4.96 (d, J = 17.1 Hz, 1H), 4.88 (d, J = 17.1 Hz, 1H), 4.47−4.50 (m, 1H), 4.31 (d, J = 15.9 Hz, 1H), 4.19 (d, J = 15.9 Hz, 1H), 3.50 (s, 3H), 3.15−3.21 (m, 2H), 2.89−2.94 (m, 2H). MS (EI) *m/z* 627.5 (M^+).

Pyridine-2-sulfonic Acid (6-Chlorobenzo[1,2,5]thiadiazol-5-ylmethyl)-[6-cyano-1-(3-methyl-3*H*-imidazol-4-ylmethyl)-1,2,3,4-tetrahydroquinolin-3-yl]amide (4l). ^{1}H NMR (300 MHz, $CDCl_3$) δ 8.75 (d, J = 7.2 Hz, 1H), 8.64 (s, 1H), 8.30 (s, 1H), 8.19 (s, 1H), 7.95−8.03 (m, 2H), 7.61−7.63 (m, 1H), 7.20 (s, 1H), 7.18 (m, 2H), 6.43 (d, J = 8.5 Hz, 1H), 4.75 (s, 2H), 4.64−4.68 (m, 1H), 4. 48 (d, J = 16.5 Hz, 1H), 4.35 (d, J = 16.5 Hz, 1H), 3.81 (s, 3H), 3.62−3.66 (m, 1H), 3.38−3.46 (m, 1H), 2.98−3.01 (m, 2H); MS (EI) *m/z* 591.4.

***N-tert*-Butyl-2-[[6-isocyano-1-(3-methyl-3*H*-imidazol-4-ylmethyl)-1,2,3,4-tetrahydroquinolin-3-yl]-(pyridine-2-sulfonyl)amino]acetamide (4m)**. ^{1}H NMR (300 MHz, CD_3OD) δ 8.93 (s, 1H), 8.71 (d, J = 7.2 Hz, 1H), 8.05 (td, J = 1.8, 7.5 Hz, 1H), 8.01−8.02 (m, 1H), 7.66 (ddd, J = 1.2, 4.8, 7.5 Hz, 1H), 7.43 (s, 1H), 7.39 (dd, J = 1.5, 8.4 Hz, 1H), 7.33 (s, 1H), 6.80 (d, J = 9.7 Hz, 1H), 4.81 (d, J = 16.8 Hz, 1H), 4.68 (d, J = 16.8 Hz, 1H), 4.32−4.44 (m, 1H), 4.00 (d, J = 17.4 Hz, 1H), 3.95 (d, J = 17.4 Hz, 1H), 3.90 (s, 3H), 3.46−3.59 (m, 2H), 3.13 (dd, J = 12, 15.3 Hz, 1H) 2.85 (dd, J = 3.3, 15.3 Hz, 1H), 1.32 (s, 9H); high-resolution mass spectroscopy (FAB+) *m/z* calcd for $C_{26}H_{32}O_3N_7S$ (MH^+) 522.2287 obsd 522.2275.

***N-tert*-Butyl-2-[[6-isocyano-1-(3-methyl-3*H*-imidazol-4-ylmethyl)-1,2,3,4-tetrahydroquinolin-3-yl]-(pyridine-3-sulfonyl)amino]acetamide (4n).** ^{1}H NMR (500 MHz, CD_3-OD) δ 9.09 (s, 1H), 8.95 (s, 1H), 8.81 (d, J = 3 Hz, 1H), 8.36 (d, J = 8.5 Hz, 1H), 7.63−7.65 (m, 1H), 7.38−7.40 (m, 2H), 7.30 (s, 1H), 6.82 (d, J = 9.5 Hz, 1H), 4.78 (d, J = 17.5 Hz, 1H), 4.62 (d, J = 17.5 Hz, 1H), 4.31−4.36 (m, 1H), 4.05 (d, J = 17 Hz, 1H), 3.97 (d, J = 17 Hz, 1H), 3.91 (s, 3H), 3.41−3.51 (m, 2H), 3.05 (dd, J = 10.5, 15.5 Hz, 1H), 2.84 (dd, J = 4, 15 Hz, 1H), 1.32 (s, 9H); high-resolution mass spectroscopy (FAB+) *m/z* calcd for $C_{26}H_{32}O_3N_7S$ (MH^+) 522.2287 obsd 522.2285.

***N-tert*-Butyl-2-[[6-isocyano-1-(3-methyl-3*H*-imidazol-4-ylmethyl)-1,2,3,4-tetrahydroquinolin-3-yl]-(pyridine-4-sulfonyl)amino]acetamide (4o).** ^{1}H NMR (500 MHz, CD_3-OD) δ 8.94 (s, 1H), 8.85 (d, J = 10 Hz, 2 H), 7.93 (d, J = 10 Hz, 2 H), 7.38−7.40 (m, 2H), 7.31 (s, 1H), 6.83 (d, J = 8.5 Hz, 1 H),), 4.76 (d, J = 17 Hz, 1H), 4.63 (d, J = 17 Hz, 1H), 4.28−4.37 (m, 1H), 4.04 (d, J = 17 Hz, 1H), 3.94 (d, J = 17 Hz, 1H), 3.94 (s, 3H), 3.42−3.52 (m, 2H), 3.05 (dd, J = 10, 15 Hz, 1H), 2.84 (dd, J = 4.5, 15 Hz, 1H), 1.32 (s, 9H); high-resolution mass spectroscopy (FAB+) *m/z* calcd for $C_{26}H_{32}O_3N_7S$ (MH^+) 522.2287 obsd 522.2284.

***N-tert*-Butyl-2-[[6-cyano-1-(3-methyl-3*H*-imidazol-4-ylmethyl)-1,2,3,4-tetrahydroquinolin-3-yl]-(4-fluorobenzenesulfonyl)amino]acetamide (4p).** ^{1}H NMR (500 MHz, CD_3OD) δ 8.94 (s, 1H), 8.03−8.00 (m, 2H), 7.39−7.37 (m, 2H), 7.35 (t, J = 8.0 Hz, 2H), 7.28 (s, 1H), 6.82 (d, J = 8.6 Hz, 1H), 4.760 (d, J = 17.0 Hz, 1H), 4.57 (d, J = 17.0 Hz, 1H), 4.26−4.24 (m, 1H), 4.01−3.85 (m, 5H), 3.49−3.46 (m, 1H), 3.34−3.33 (m, 1H), 3.03−2.97 (m, 1H), 2.80−2.79 (m, 1H), 1.35 (s, 9H), MS (EI) *m/z* 539.4 (M^+).

***N-tert*-Butyl-2-[[6-cyano-1-(3-methyl-3*H*-imidazol-4-ylmethyl)-1,2,3,4-tetrahydroquinolin-3-yl]-(1-methyl-1*H*-imidazole-2-sulfonyl)amino]acetamide (4q).** ^{1}H NMR (300 MHz, CD_3OD) δ 8.94 (s, 1H), 7.44 (s, 1H), 7.39 (d, J = 1.2, 5.1 Hz, 1H), 7.37 (s, 1H), 7.32 (d, J = 0.9 Hz, 1H), 7.11 (s, 1H), 6.84 (d, J = 5.4 Hz, 1H), 4.79 (d, J = 10.8 Hz, 1H), 4.66 (d, J = 10.8 Hz, 1H), 4.39−4.43 (m, 1H), 4.05 (s, 2 H), 3.94 (s, 3H), 3.91 (s, 3H), 3.52−3.61 (m, 2H), 3.04−3.11 (m, 2H), 1.3 (s, 9 H); MS (EI) *m/z* 525.5 (M^+).

Biological Assays. *Plasmodium* Strains. The *P. falciparum* strains used in this study were 3D7, W2, K1, HB3, and Dd2. 3D7 was used for all ED_{50} determinations except in Table 2. All strains were obtained from the MR4 Unit of the American Type Culture Collection (ATCC, Manassas, VA), except 3D7, which was provided by Dr. Pradipsinh Rathod from the University of Washington. The *P. berghei* isolate NK65 used for the in vivo experiment and was also obtained from the ATCC.

***P. falciparum* Culture.** Strains of *P. falciparum* were sustained in vitro based on experimental techniques as described by Trager and Jensen.[25] Cultures were maintained in RPMI-1640 (Sigma, St. Louis, MI) with 2 mM L-glutamine, 25 mM HEPES, 33 mM $NaHCO_3$, 20 μg/mL gentamicin sulfate, and 20% (v/v) heat-inactivated human plasma type A+ (RP-20P). Type A+ erythrocytes were obtained from lab donors, washed three times with RPMI, resuspended in 50% RPMI, and stored at 4 °C. Parasites were grown in 10 mL of a 2% hematocrit/RP-20P (v/v) in 50-mL flasks under a 5% CO_2, 5% O_2, and 90% N_2 atmosphere.

***P. falciparum* ED_{50} Determination.** One microliter of PFTI dissolved in DMSO was added to each well of a 96-well plate followed by the addition of 200 μL of an asynchronous *P. falciparum* culture at parasitemia and hematocrit of 0.5%. Plates were flushed with 5% CO_2, 5% O_2, and 90% N_2 and then incubated at 37 °C for 48 h. [8-^{3}H]-hypoxanthine (0.3 μCi, 20 Ci/mmol, American Radiolabeled Chemicals) in 30 μL of RP-20P was added to cultures and incubated for an additional 24 h. Cells were harvested onto filter mats by a Multiharvester (Skatron, Sunnyvale, CA), and the radioactivity incorporated into the parasites was counted on a beta-scintillation counter. The background level detected with uninfected erythrocytes was subtracted from the data. The ^{3}H-incorporation into infected RBCs with 1 μL of DMSO vehicle alone represents 100% malaria growth. ED_{50} values were determined by linear regression analysis of the plots of ^{3}H-hypoxanthine incorporation versus concentration of compound. Each compound was tested at least twice, and the mean value is shown; individual measurements differed by less than 3-fold.

PfPFT and Rat PFT IC_{50} Determination. The PFT assay used to determine the IC_{50}s of the compounds used a scintillation proximity assay (SPA) kit (Amersham Biosciences, Piscataway, NJ) as previously described,[7] with the modifications as noted below. Partially purified PfPFT[7] or recombinant rat PFT[26] was prepared as previously described. Incubation of the reaction was shortened to 15 min at 37° C for Rat-PFT in order to remain in the linear portion of the enzyme kinetics curve. The activity for Pf-PFT was determined using 1.0 μM biotinylated lamin B peptide substrate (biotin-YRASNR-SCAIM) and 0.01 μM of the same peptide substrate for the rat PFT. IC_{50} values were calculated using linear regression analysis of the plots of ^{3}H−FPP prenylation vs concentration of compounds. Each compound was tested at least twice and the mean value is shown; individual measurements differed by less than 50%.

Radiolabeling of *P. falciparum* Prenylated Proteins. *P. falciparum* 3D7 cells in RBC (1% asynchronous parasitemia, 2% hematocrit) were cultured for 48 h in 2 mL RP-20P containing 5 μCi (42 nM) of [1-^{3}H]farnesol or [1-^{3}H]geranylgeraniol ([^{3}H]GGOH) (both 15 Ci/mmol, American Radiolabeled Chemicals Inc.), with the indicated concentrations of PFTI **4a** (Figure 3) or 0.6, 1.5, and 5 times the ED_{50} (1.8 μM, 4.5 μM, & 15 μM) concentration of **6** (data not shown). The parasite cells were isolated from RBCs by the saponin treatment as described.[7] Radiolabeled malarial proteins (30 μg/lane by Bradford protein assay) were resolved on a 12.5% SDS−PAGE gel and visualized by fluorography. The gel was exposed to X-ray film at − 80 °C for 5 days.

Immunofluorescence Microscopy. The **PFTI 4b** was added to synchronized *P. falciparum* 3D7 cultures at the ring stage (6 h post-synchronization). Parasites were synchronized using 5% sorbitol.[27] Images of stained thin smears of the culture at different time points were captured with a Nikon TE200 inverted microscope equipped with Spot digital camera for indirect immunofluorescence microscopy.[7] Fixed cells were probed with affinity-purified polyclonal rabbit anti-farnesyl antibody (Calbiochem**,** 1:50) and goat anti-rabbit IgG Alexafluor-555-conjugated antibody (Molecular Probes, Inc., 1:200). Nuclei were stained with 1 μM 4′,6-diamidino-2-phenylindole (DAPI). The fluorescent images were captured with a DeltaVision image restoration microscope system (Applied Precision) equipped with a Photometrix cooled CCD camera. The captured images were deconvolved with the SoftWoRx software. Immunofluorescence analyses of prenylated proteins of parasite cultures treated with PFTI for different durations were done using identical experimental conditions.

PFTI Cytotoxicity Experiments. In 24-well plates, 1-mL cultures *P. falciparum* at 0.5% asynchronous parasitemia and 1.0% hematocrit were treated with 22.5 and 225 nM of **PFTI 4b**, 3 and 30 times the ED_{50} for this compound, respectively. Cultures lacking drug were used as controls. Separate cultures were set up for 24, 48, 72, 96, and 168 h drug exposure, at which time infected RBCs were washed three times and resuspended in fresh RPMI without compound. To monitor for growth after cultures had potentially overgrown, replicate cultures at 72 h were diluted 1:10 into fresh RPMI with or without drug at 1% hematocrit for the 96 and 168 h time points. Media was replaced on alternate days, and fresh erythrocytes at 1% hematocrit were added on opposite days of media replacement. *P. falciparum* growth was followed by microscopy.

Studies with *P. berghei*-Infected Mice. Five female Balb/C mice (6−8 weeks old) were used per group in these experiments. Two groups received **PFTI 4a** at delivery rates of 200 mg/kg/day and 40 mg/kg/day via a subcutaneously implanted osmotic pump (#1007D, Alzet, Cupertino, California) for 7 days. For the 200 mg/kg/day pump, 33.3 mg of **4a** in

100 μL of DMSO:H_2O (1:1) was loaded in the pump, which was implanted into 20 g mice. The 40 mg/kg/day pump was loaded similarly with 6.5 mg of compound. The pumps are designed to deliver 0.5 μL/h and 84% of the total solution over 7 days. For the two different control groups, mice received pumps with vehicle alone (DMSO:water) or no pumps. All mice were infected by intraperitoneal injection with 10^6 parasitized RBC, *P. berghei* NK65, 4 h after implantation of the pumps. Parasitemia was determined by light microscopy of blood samples, and mice were euthanized upon reaching 50% parasitemia.

Acknowledgment. This work was supported by grants from the Medicines for Malaria Venture, support from the W.M. Keck Foundation Center for Microbial Pathogens at the University of Washington, and grants from the National Institutes of Health (AI054384 to M.H.G, AI043679 to D.C., and CA67771 to SMS and A.D.H.). We are grateful to S. Rosenberg (Abbott), D. Heimbrook (Merck), and D.W End (Janssen) for supplying PFT inhibitors, and to Martin Sadilek for help with LC-MS determination of PFTI blood level.

Appendix

Abbreviations: PFT: protein farnesyltransferase; PFTIs: PFT inhibitors; *P. falciparum: Plasmodium falciparum*; PfPFT: *P. falciparum* PFT; RBC: red blood cells; FPP: farnesyl pyrophosphate; PGGT: protein geranylgeranyltransferase; THQ: tetrahydroquinoline; ED_{50}: effective dose that inhibits 50% of *P. falciparum* proliferation; IC_{50}: inhibitor concentration that inhibits 50% of PFT enzymatic activity; BMS: Bristol-Myers Squibb.

Supporting Information Available: HR-MS spectral data. This material is available free of charge via the Internet at http://pub.acs.org.

References

(1) www.mmv.org. 2003.
(2) Gelb, M. H.; Hol, W. G. Parasitology. Drugs to combat tropical protozoan parasites. *Science* **2002**, *297*, 343−344.
(3) Leonard, D. M. Ras farnesyltransferase: a new therapeutic target. *J. Med. Chem.* **1997**, *40*, 2971−2990.
(4) Cox, A. D.; Der, C. J. Ras family signaling: therapeutic targeting. *Cancer Biol. Ther.* **2002**, *1*, 599−606.
(5) Sebti, S. M.; Hamilton, A. D.; Moffitt, H. L. *Farnesyltransferase Inhibitors in Cancer Therapy*; Humana Press: Totowa, NJ, 2001.
(6) Yokoyama, K.; Goodwin, G. W.; Ghomashchi, F.; Glomset, J.; and Gelb, M. H. Protein prenyltransferases. *Biochem. Soc. Trans.* **1992**, *20*, 489−494.
(7) Chakrabarti, D.; Da Silva, T.; Barger, J.; Paquette, S.; Patel, H.; Patterson, S.; Allen, C. M. Protein farnesyltransferase and protein prenylation in Plasmodium falciparum. *J. Biol. Chem.* **2002**, *277*, 42066−42073.
(8) Chakrabarti, D.; Azam, T.; DelVecchio, C.; Qiu, L.; Park, Y. I.; Allen, C. M. Protein prenyl transferase activities of Plasmodium falciparum. *Mol. Biochem. Parasitol.* **1998**, *94*, 175−184.
(9) www.plasmodb.org. 2003.
(10) Lombardo, L. J.; Camuso, A.; Clark, J.; Fager, K.; Gullo-Brown, J.; Hunt, J. T.; Inigo, I.; Kan, D.; Kolowitz, B.; Lee, F.; McGlinchey, K.; Qian, L.; Ricca, C.; Rovnyak, G.; Traeger, S.; Tokarski, J.; Williams, D. K.; Wu, L. I.; Zhao, Y.; Manne, V.; Bhide, R. S. Design, synthesis and structure−activity relationships of tetrahydroquinoline-based farnesyltransferase inhibitors. *Bioorg. Med. Chem. Lett.* **2005**, *15*, 1895−1899.
(11) Chen, B.-C.; Sundeen, J. E.; Guo, P.; Bednarz, M. S.; Zhao, R. Novel triethylsilane mediated reductive *N*-alkylation of amines: improved synthesis of 1-(4-imidazolyl)methyl-4-sulfonylbenzodiazepines, new farnesyltransferase inhibitors. *Tetrahedron Lett.* **2001**, *42*, 1245−1246.
(12) Gwaltney, S. L.; O'Connor, S. J.; Nelson, L. T.; Sullivan, G. M.; Imade, H.; Wang, W.; Hasvold, L.; Li, Q.; Cohen, J.; Gu, W. Z.; Tahir, S. K.; Bauch, J.; Marsh, K.; Ng, S. C.; Frost, D. J.; Zhang, H.; Muchmore, S.; Jakob, C. G.; Stoll, V.; Hutchins, C.; Rosenberg, S. H.; Sham, H. L. Aryl tetrahydropyridine inhibitors of farnesyltransferase: bioavailable analogues with improved cellular potency. *Bioorg. Med. Chem. Lett.* **2003**, *13*, 1363−1366.
(13) Hunt, J. T.; Ding, C. Z.; Batorsky, R.; Bednarz, M.; Bhide, R.; Cho, Y.; Chong, S.; Chao, S.; Gullo-Brown, J.; Guo, P.; Kim, S. H.; Lee, F. Y.; Leftheris, K.; Miller, A.; Mitt, T.; Patel, M.; Penhallow, B. A.; Ricca, C.; Rose, W. C.; Schmidt, R.; Slusarchyk, W. A.; Vite, G.; Manne, V. Discovery of (*R*)-7-cyano-2,3,4,5-tetrahydro-1-(1*H*-imidazol-4-ylmethyl)-3-(phenylmethyl)-4-(2-thienylsulfonyl)-1*H*-1,4-benzodiazepine (BMS-214662), a farnesyltransferase inhibitor with potent preclinical antitumor activity. *J. Med. Chem.* **2000**, *43*, 3587−3595.
(14) End, D. W.; Smets, G.; Todd, A. V.; Applegate, T. L.; Fuery, C. J.; Angibaud, P.; Venet, M.; Sanz, G.; Poignet, H.; Skrzat, S.; Devine, A.; Wouters, W.; Bowden, C. Characterization of the antitumor effects of the selective farnesyl protein transferase inhibitor R115777 in vivo and in vitro. *Cancer Res.* **2001**, *61*, 131−137.
(15) Bell, I. M.; Gallicchio, S. N.; Abrams, M.; Beshore, D. C.; Buser, C. A.; Culberson, J. C.; Davide, J.; Ellis-Hutchings, M.; Fernandes, C.; Gibbs, J. B.; Graham, S. L.; Hartman, G. D.; Heimbrook, D. C.; Homnick, C. F.; Huff, J. R.; Kassahun, K.; Koblan, K. S.; Kohl, N. E.; Lobell, R. B.; Lynch, J. J., Jr.; Miller, P. A.; Omer, C. A.; Rodrigues, A. D.; Walsh, E. S.; Williams, T. M. Design and biological activity of (*S*)-4-(5-([1-(3-chlorobenzyl)-2-oxopyrrolidin-3-ylamino]methyl)imidazol-1-ylmethyl)benzonitrile, a 3-aminopyrrolidinone farnesyltransferase inhibitor with excellent cell potency. *J. Med. Chem.* **2001**, *44*, 2933−2949.
(16) Taveras, A. G.; Kirschmeier, P.; Baum, C. M. Sch-66336 (sarasar) and other benzocycloheptapyridyl farnesyl protein transferase inhibitors: discovery, biology and clinical observations. *Curr. Top. Med. Chem.* **2003**, *3*, 1103−1114.
(17) Ohkanda, J.; Knowles, D. B.; Blaskovich, M. A.; Sebti, S. M.; Hamilton, A. D. Inhibitors of protein farnesyltransferase as novel anticancer agents. *Curr. Top. Med. Chem.* **2002**, *2*, 303−323.
(18) Carrico, D.; Ohkanda, J.; Kendrick, H.; Yokoyama, K.; Blaskovich, M. A.; Bucher, C. J.; Buckner, F. S.; Van Voorhis, W. C.; Chakrabarti, D.; Croft, S. L.; Gelb, M. H.; Sebti, S. M.; Hamilton, A. D. In vitro and in vivo antimalarial activity of peptidomimetic protein farnesyltransferase inhibitors with improved membrane permeability. *Bioorg. Med. Chem.* **2004**, *12*, 6517−6526.
(19) Eastman, R. T.; White, J.; Hucke, O.; Bauer, K.; Yokoyama, K.; Nallan, L.; Chakrabarti, D.; Verlinde, C. M. J.; Gelb, M. H.; Rathad, P. K.; Van Voorhis, W. C. Resistance to a protein farnesyltransferase inhibitor in *Plasmodium falciparum*. *J Biol. Chem.* **2005**, *280*, 13554−13559.
(20) Vennerstrom, J. L.; Arbe-Barnes, S.; Brun, R.; Charman, S. A.; Chiu, F. C.; Chollet, J.; Dong, Y.; Dorn, A.; Hunziker, D.; Matile, H.; McIntosh, K.; Padmanilayam, M.; Santo, T. J.; Scheurer, C.; Scorneaux, B.; Tang, Y.; Urwyler, H.; Wittlin, S.; Charman, W. N. Identification of an antimalarial synthetic trioxolane drug development candidate. *Nature* **2004**, *430*, 900−904.
(21) Wiesner, J.; Kettler, K.; Sakowski, J.; Ortmann, R.; Katzin, A. M.; Kimura, E. A.; Silber, K.; Klebe, G.; Jomaa, H.; Schlitzer, M. Farnesyltransferase inhibitors inhibit the growth of malaria parasites in vitro and in vivo. *Angew. Chem., Int. Ed* **2004**, *43*, 251−254.
(22) Angibaud, P. R.; Vanet, M. G.; Filliers, W.; Broecks, R.; Ligny, Y. A.; Muller, P.; Poncelet, V. S.; End, D. W. Synthesis Routes Towards the Farnesyl Protein Transferase Inhibitor Zarnestra. *Eur. J. Org. Chem.* **2004**, 479−486.
(23) Ohkanda, J.; Buckner, F. S.; Lockman, J. W.; Yokoyama, K.; Carrico, D.; Eastman, R.; Luca-Fradley, K.; Davies, W.; Croft, S. L.; Van Voorhis, W. C.; Gelb, M. H.; Sebti, S. M.; Hamilton, A. D. Design and synthesis of peptidomimetic protein farnesyltransferase inhibitors as anti-*Trypanosoma brucei* agents. *J. Med. Chem.* **2004**, *47*, 432−445.
(24) Corey, E. J.; Posner, G. H.; Atkinson, R. F.; Wingard, A. K.; Halloran, D. J.; Radzik, D. M.; Nash, J. J. Formation of Olefins Via Pyrolysis of Sulfonate Esters. *J. Org. Chem.* **1989**, *54*, 389−393.
(25) Trager, W. and Jensen, J. B. Human malaria parasites in continuous culture. *Science* **1976**, *193*, 673−675.
(26) Yokoyama, K.; Zimmerman, K.; Scholten, J.; Gelb, M. H. Differential prenyl pyrophosphate binding to mammalian protein geranylgeranyltransferase-I and protein farnesyltransferase and its consequence on the specificity of protein prenylation. *J Biol. Chem.* **1997**, *272*, 3944−3952.
(27) Lambros, C. and Vanderberg, J. P. Synchronization of Plasmodium falciparum erythrocytic stages in culture. *J. Parasitol.* **1979**, *65*, 418−420.

JM0491039